The College of Engineering
University of Wisconsin-Madison

DARK-MANTLE MATERIAL AS A SOURCE OF HELIUM

WCSAR-TR-AR3-8810-3

Technical Report

**Wisconsin Center for
Space Automation and Robotics**

•

**A NASA supported Center for
the Commercial Development of Space**

DARK-MANTLE MATERIAL AS A SOURCE OF HELIUM

WCSAR-TR-AR3-8810-3

E.N. Cameron

Wisconsin Center for Space Automation and Robotics
University of Wisconsin
1500 Johnson Drive
Madison WI 53706

January 1988

WCSAR-TR-AR3-8810

January 28, 1988

Memorandum to G. L. Kulcinski

From E. N. Cameron

Dark-mantle material as a source of helium

Introduction

At the suggestion of Dr. Paul C. Spudis, of the U. S. Geological Survey, I have undertaken a review of information regarding the nature and distribution of the dark-mantle material that covers certain sizable areas of the lunar nearside, with the purpose of evaluating the material as a possible source of helium. Dr. Spudis points out that the essential component of the material is glass, which occurs as tiny spherules (mean diameter in the neighborhood of 40 μm), that the material is considered to be volcanic ash, and that it occurs in deposits that may be as much as tens of meters in thickness, at least over certain areas. Information available from photography and from back-scattering radar surveys indicates that areas covered by such material are free or nearly free of blocks. Such material would be easily minable and might require no beneficiation.

This memorandum presents the results of a survey of pertinent literature. Information, papers. and maps furnished by Dr. Spudis have greatly facilitated the study. There is a considerable literature on the dark-mantle material; references cited below are principal sources of information.

Distribution of dark-mantle material

Principal areas of dark-mantle are shown in Figure 1. The largest areas are the one along the south and southwest sides of Mare Serenitatis, including the Taurus-Littrow and Sulpicius Gallus regions, and the Rima Bode area. Dark-mantle material typically occurs along the margins of maria. It forms blanket-like deposits that extend from the mare out over adjacent highland areas, burying or partly burying some of the topographic features of the highlands. On telescopic spectral reflectance maps, the dark-mantle areas are darker than the maria, hence their name. The spectral reflectance of dark-mantle areas of Mare Serenititas, including the Taurus-Littrow area, has been investigated by Adams et al. (1974). Their work is discussed below.

The Apollo 17 mission landed on the floor of the Taurus-Littrow valley. Owing to the surveys done and the numerous samples taken during that mission, it is the principal source of information on the mineralogy, petrology, chemistry, and helium content of dark-mantle material. The information has been used by various investigators as a basis for interpreting other dark-mantle material marginal to Mare Serenitatis.

The Taurus-Littrow Valley and Mare Serenitatis

On the pre-mission maps of the Taurus-Littrow area (Scott et al., 1972), the valley floor on which Apollo 17 landed is shown as largely covered by dark-mantle material, and dark-mantle material is depicted as extending over a much larger area to the north and west, overlapping the boundary between highland terrain and Mare Serenitatis. The valley

floor was sampled at a number of points during the Apollo 17 mission. Study of the samples showed that the regolith consists largely of basaltic debris produced by gardening of the underlying high-Ti subfloor basalt. Admixed, however, are droplets of orange and black glass in amounts ranging from 3.1 to 27.1 percent (Heiken amd McKay, 1974) in the 90 to 150 μm fractions of the samples. Heiken and McKay concluded, from petrographic studies of the samples, "that the dark mantle, at the Apollo 17 site, is regolith developed on a sequence of interbedded mare lava and orange glass deposits. Although containing fragments of glass, which may have a pyroclastic origin, the dark mantle itself does not have a pyroclastic origin". However, Wolfe et al. (1981) concluded that the orange and black glass droplets (the glass "fragments" of Heiken and McKay) represent a deposit of volcanic ash overlying the topmost mare flow at the Apollo 17 site and admixed with basaltic debris by gardening. Wilhelms (1987) expressed a similar conclusion. Elsewhere in the Taurus-Littrow amd Mare Serenitatis regions there is a younger mare basalt that overlaps older basalts and the ash deposits (Lucchitta and Schmitt, 1974). Wolfe et al. observe that the work of Heiken and McKay indicates that in 19 samples of dark regolith from the valley floor orange and black glass droplets average 10.6 percent of the 90-150 μm fraction and that the ash deposit must therefore have been extensive.

Pure volcanic ash was found only in a trench excavated in the rim of Shorty Crater and in cores from two drive tubes put down at a point beside the trench. The material has been interpreted as a clod ejected from a subsurface layer of ash at least 70 cm thick. In the trench the

pure ash (orange soil, sample 74220) consists almost entirely of orange glass droplets containing 8.09% TiO2 (Wänke et al.), 1973)) to 8.96 TiO2 (Nava, 1974). The helium content of this material (Hintenberger et al., 1974) is reported as 2.6 wppm, not 26 wppm as erroneously stated in my earlier report of 9/1/87.

The core from the upper of the two drive tubes is designated as sample 74002, that from the lower tube as sample 74001. The section given by the two drive tubes shows a downward progression from orange ash at the top to black ash at the bottom. The black ash consists largely of droplets of black glass produced by devitrification of orange glass. A portion of the black ash analyzed by Heiken and McKay (1974) showed 10.34 TiO2 and contained 8 percent orange glass, 73.3 percent black glass, and 16.6 percent brown glass. Subsequently Nagle (1978) examined the cores and found a layered succession of 6 units in 74001, overlain by an additional 3 units of 74002 (Fig. 2).

The cores have been studied intensively since 1974. McKay et al. (1978) sieved portions of each of 14 samples into 8 size fractions. Above a depth of 5.5 cm. the material shows evidence (agglutinates, lithic fragments, and mineral fragments) of gardening over a period of about 10 m. y. Below 5.5 cm. the materials are composed solely of droplets of glass, ranging in mean grain size from 36 to 52 μm. Heiken and McKay showed that the ratio of crystalline droplets to homogeneous glass droplets (orange glass) plus partly crystalline droplets changes downward from about 0.5 to 1 to about 14 to 1 (Figure 3) at the bottom of the section sampled by the drive tubes.

Splits of the sieve fractions of samples were furnished by the McKay group to Bogard and Hirsch, who determined He (1978) in two or more sieve fractions of each of 15 samples distributed from top to bottom of the drive tube section (Table 1). For most of the samples, only the 150-250 and -20 μm fractions were analyzed. Enrichment of the finer fraction in He is shown by every sample. Samples from the upper reworked (gardened) 5.5 cm of the section are richest in He. Below that depth the He contents are much less. However, even in the richest samples above 5.5 cm, the 4He content of the -20μm fraction is only 8 wppm. Below 5.5 cm the 4He content is 0.9 wppm or less.

Heiken and McKay (1974) and Haggerty (1974) have shown that the black droplets consist largely of olivine, ilmenite, and residual glass. Given the TiO2 content of the original glass, the ilmenite content of the devitrified glass could conceivably approach 20 percent. To the extent that the ilmenite crystallites occur at the outer edges of the droplets, then in view of the high He retentivity of ilmenite, an ash composed largely of black glass should have a higher He content than glass composed of orange glass. This is obviously not the case in the material of the rim of Shorty crater. The answer may be that the black ash there has been effectively shielded from the solar wind by the overlying orange ash during the relatively short period of about 19 m.y. (Eugster et al., 1977) since the impact that created Shorty Crater. If this is true, the samples of ash from Apollo 17 cannot be taken as indicative of the He content of black ash in areas where the ash has

been exposed to the solar wind by gardening over the period of more than 3 b. y. since the ash deposits were formed (Eugster et al., 1979).

The above is important, because Adams et al. (1974) concluded from spectral reflectance studies of dark mantle and sample 74001 that the dark spheres (i. e., black glass droplets) found in sample 74001 are the characteristic component of dark-mantle material.

A note of caution is necessary at this point. It is not be expected that devitrification of orange glass, aapparently the original form of ash deposited, will be uniform over substantial areas. Various stages of devitrification have already been found in various samples, and this must be taken into account. Haggerty (p. 194) remarks: "Initiation of crystallization in the orange glass imparts to it a distinct black-body effect, and this effect results in progressively higher degrees of opacity as the ratio of non-crystalline to crystalline material decreases. The subtleties of fine contrast regolith mapping or of photogeologic interpretation (Lucchitta and Schmitt, 1974) of the extent of the orange soil therefore depend in large measure on the degree of devitrification. The same is true for predictions based on telescopic reflectance observations". Just as important from the standpoint of recovery of helium is that if the helium content of the volcanic ash is a function of ilmenite content, helium content can be expected to vary over an appreciable range.

Adams et al. (1974) concluded that dark-mantle material derived from volcanic ash is of broad extent alomg the southern and southwestern sides of Serenitatis, including the Sulpicius Gallus area, and several

other areas of the lunar nearside (see Figure 1). Those areas, as pointed out by Dr. Spudis, are free or nearly free of blocks, and in parts of them the deposits of ash may be tens of meters in thickness. Such features, together with the fine grain size of the ash, would greatly simplify mining of regolith and recovery of helium. On the other hand, the internal structure of the ash deposits may be unfavorable. Information on this point is mainly from an analysis of photographs of the Sulpicius Gallus region by Lucchitta and Schmitt (1974). Those authors state (p. 233): "It is our conclusion that the Sulpicius Gallus and Taurus-Littrow deposits of orange, red, black and dark mantle formed as locally stratified but discontinuous pyroclastic deposits produced by multiple 'fire fountain' eruptions during the later stages of accumulation of the older mare basalt units". Such a structure could greatly complicate exploration, sampling, and mining. Finally, while it is evident that thick deposits of ash are present in certain areas, only the uppermost portions of such deposits will have been gardened and exposed to the solar wind.

In summary, pyroclastic deposits of Serenitatis and Taurus-Littrow comprise both orange glass and black glass, the latter derived from the former by devitrification. The helium content of orange glass is very low. The helium content of black glass that has been exposed to the solar wind for long periods of time is unknown. It may be high where devitrification is advanced but will be lower where devitrification is incomplete. Whether large bodies of ash of acceptable helium content might be delineated will not be known until extensive exploration and

sampling have been done. The complexity of structure sugggested by the work of Lucchitta and Schmitt is not encouraging. In addition, given the nature of the process of devitrification, it seems probable that substantial variation in grade both laterally and vertically will be found within individual bodies of ash. In areas such as Taurus-Littrow where the ash deposits were apparently thin, the problem of gardening and dilution of ash by underlying material must be considered. Where the subfloor consists of high-Ti basalt, dilution will probably be no problem, since regolith derived from such basalt is likely to be high in helium, but where ash overlies highland material, dilution will have caused substantial lowering of grade, since regolith developed on highland material is low in helium content.

Volcanic ash at the Apollo 15 site

I have reviewed the literature dealing with the occurrence of volcanic glass at the Apollo 15 landing site. I will summarize existing information in a later memorandum and will note here only that there is nothing to indicate the presence of ash deposits high in helium in that area. Glass of several types is apparently widespread in the area but is present in amounts of only 10% or less of the regolith.

Recommendations

Black ash fractions separated from other samples of the dark-mantle material of Taurus-Littrow should also be analyzed for helium in the hope that they will indicate something of the range of variation in the helium content of black glass. Specifically, samples 70008, 220, 235, and 239 are reported by Heiken and McKay (1974) to contain respectively

12%, 11% and 15% black glass in the 90-150 μm fraction. They also report 11.6% black glass in the same fraction of sample 75111,13. Beyond this, no further work is recommended pending a landing mission on the moon, one that will involve detailed exploration and sampling. Remote sensing cannot resolve the problems summarized above.

For the present, in view of the uncertainties as to the grade and structure of the volcanic ash deposits, I recommend that AR-3 continue to focus on the maria regoliths as potential sources of helium, against the contingency that volcanic ash deposits will not be found to be suitable sources. However, it would be unwise, in view of the limited nature of present information, to rule out the dark-mantle areas as potential sources of helium; in fact, I would recommend systematic exploration and sampling of the appropriate areas of Serenitatis. If future exploration indicates that obtaining large amounts of helium from volcanic ash deposits is feasible, methods of mining and processing maria regoliths could be easily adapted to volcanic ash deposits. Estimates of energy and dollar costs based on mining of the maria would surely be conservative if applied to mining ash deposits.

REFERENCES

Adams, J. B., C. Pieters, and T. B. McCord, 1974, Orange glass: Evidence for regional deposits of pyroclastic origin on the moon. Fifth Lunar Sci. Conf., Proc., vol. 1, pp. 171-186.

Bogard, D. D., and W. C. Hirsch, 1978, Depositional and irradiational history and noble gas content of orange-black droplets in the

74001/2 core from Shorty Crater. Ninth Lunar Sci. Conf., Proc., pp. 1981-2000.

Eugster, O., P. Eberhardt, J. Geiss, N. Grögler,, M. D. Mendia, and M. Mörgeli, 1977, The cosmic ray exposure history of Shorty Crater samples; the age of Shorty Crater. Eighth Lunar Sci. Conf., Proc., pp. 3058-3082.

Eugster, O., N. Grogler, P. Eberhardt,, and J. Geiss, 1979, Double drive tube 74001/2: History of the black and orange glass; determination of a pre-exposure 3.7 AE age by Xe-136/U-235 dating. Tenth Lunar Sci. Conf., Proc., pp. 1351-1379.

Haggerty, S. E., 1974, Apollo 17 orange glass: textural and morphological characteristics of devitrification. Fifth Lunar Science Conf., Proc., vol. 1, pp. 193-206.

Head, J. W., 1974, Lunar dark-mantle deposits: Possible clues to the distribution of early mare deposits. Fifth Lunar Sci. Conf., Proc., vol. 1, pp. 207-222.

Heiken, G. H., and D. S. McKay, 1974, Petrography of Apollo 17 soils. Fifth Lunar Sci. Conf., Proc., vol. 1, pp 843-860.

Heiken, G. H., and D. S. McKay, 1978, Petrology of a sequence of pyroclastic rocks from the valley of Taurus-Littrow (Apollo 17 landing site). Ninth Lunar Planet. Sci. Conf., Proc., pp. 1933-1943.

Lucchitta, B. K., 1973, Photogeology of the dark material in the Taurus-Littrow region of the moon. Fourth Lunar Sci. Conf., Proc., vol. 1, pp. 149-162.

Lucchitta, B. K., and H. Schmitt, 1974, Orange material in the Sulpicius Gallus Formation of the southwestern edge of Mare Serenitatis. Fifth Lunar Sci. Conf., Proc., vol. 1, pp. 221-274.

Nagle, J. S., 1978, Drive tubes 74002/74001: Dissection and description. Lunar Core Catalog, NASA Johnson Space Center, Houston, Supplement VIII.5.i, 49 pp.

Nava, D. F., 1974, Chemical compositions of some soils and rock types from the Apollo 15, 16, and 17 lunar sites. Fifth Lunar Sci. Conf., Proc., vol. 2, pp. 1087-1096.

Pieters, C., T. B. McCord, M. P. Charette, and J. B. Adams, 1974, Lunar surface identification of the dark mantling material in the Apollo 17 soil samples. Science, vol. 183, pp. 1191-1196.

Scott, D. H., B. K. Lucchitta, and M. H. Carr, 1972, Geologic maps of the Taurus-Littrow region of the moon. U. S. Geol. Survey, Map 1-800.

Wänke, H., H. Baddenhausen, G. Dreibus, E. Jagoutz,, H. Kruse, H. Palme, B. Spettel, and F. Teschke, 1973, Multielement analyses of Apollo 15, 16, and 17 samples and the bulk composition of the moon. Fourth Lunar Sci. Conf., Proc., vol. 2, pp. 1461-1481.

Wilhelms, Don E., 1987, The geologic history of the moon. U. S. Geol. Survey, Prof. Paper 1348, 302 pp.

Wolfe, E. W., N. C. Bailey, B. K. Lucchitta, W. R. Muehlberger, D. H. Scott, R. L. Sutton, and H. C. Wilshire, 1981, The geologic investigation of the Taurus-Littrow Valley: Apollo 17 landing site. U. S. Geological Survey, Prof. Paper 1080-C, 280 pp.

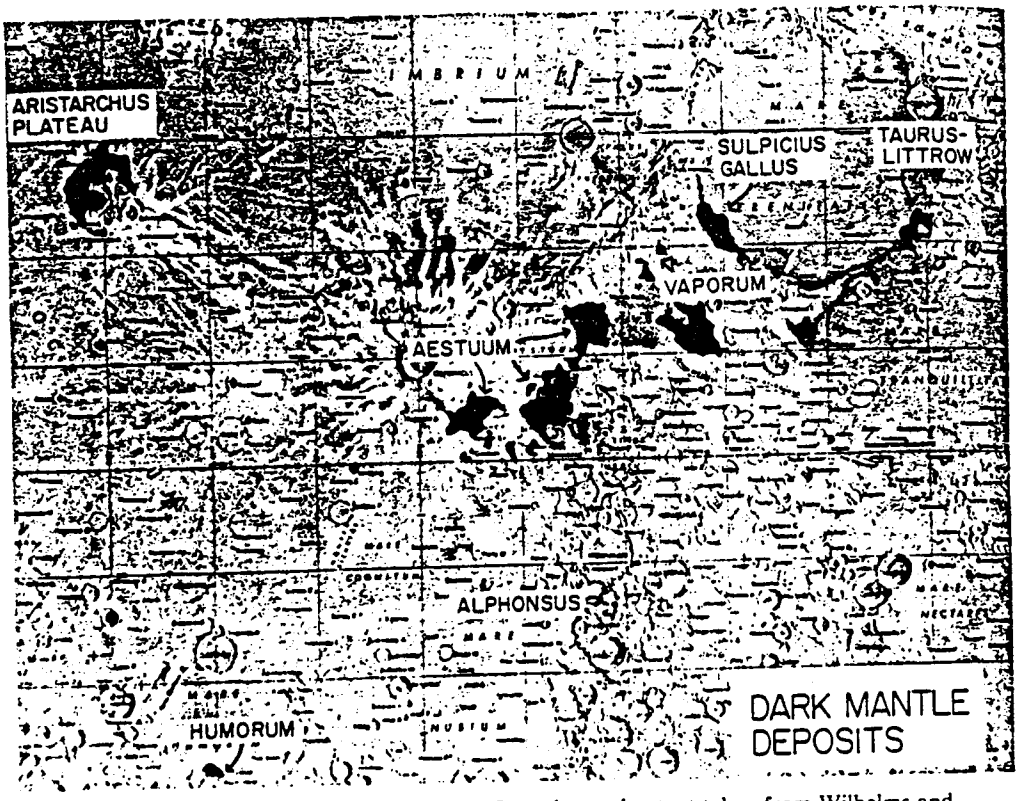

Fig. 1 Major lunar dark-mantle deposits. Location and extent taken from Wilhelms and McCauley (1971).

From Head (1974)

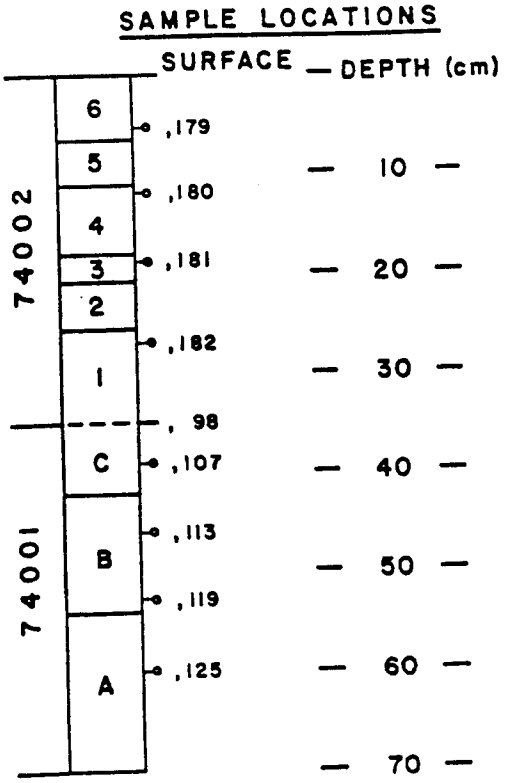

Sample locations and major depositional units of Nagle (1978).

Figure 2. From Heiken and McKay (1978).

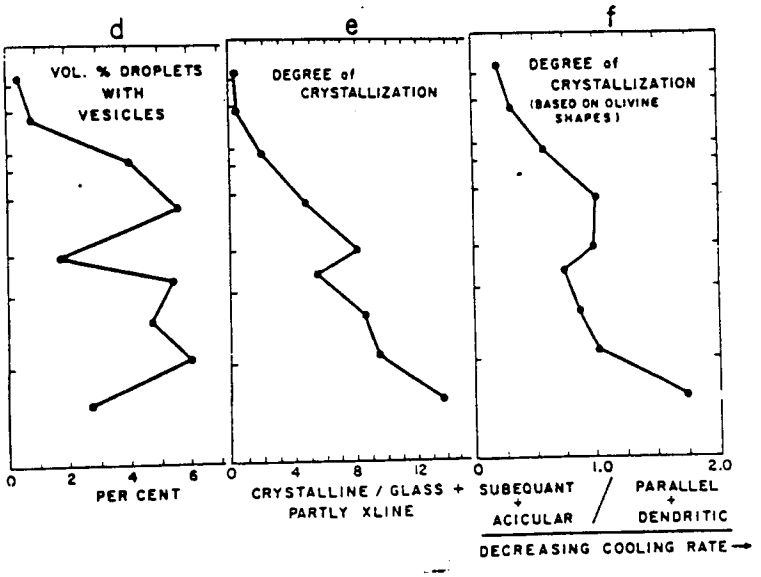

Figure 3. Part of Figure 2 of Heiken and McKay (1978). (e) Ratio of crystalline to glass plus partly crystalline droplets in 74001/74002. This ratio is roughly equal to the ratio of "black" to orange glass.

Table 1. Isotopic concentrations (units of cm^3 STP/g) and ratios of noble gases in grain size separates of soils from the 74002-74001 drive tube. Subsurface soil depths are also indicated. Absolute uncertainties in concentrations are estimated as +5-10% for He, Ne, and Ar and ±10-15% for Kr and Xe. Relative uncertainties given for isotopic ratios are one sigma of the mean of multiple measurements of individual ratios plus one-half the applied blank corrections. Absolute isotopic ratios have an additional uncertainty of ±0.1%/mass unit in applied discrimination corrections. Blank corrections for <20 μm grain sizes were: $^4He \gtrsim 1\%$, $^{22}Ne \gtrsim 2\%$, $^{36}Ar \leq 1\%$, and $^{40}Ar \gtrsim 2\%$, except for soil 74001,113 which had somewhat higher blank corrections. Blank corrections for 150-250 μm grain sizes were generally: $^4He \leq 15\%$, $^{22}Ne \leq 25\%$, $^{36}Ar \gtrsim 26\%$, and $^{40}Ar \leq 6\%$. Soil 74001,113 again showed somewhat higher blank corrections and was the only exception to the above limits for He and Ar blanks.

Sample	Wt. (mg)	^3He ×10^{-7}	^4He ×10^{-4}	^{22}Ne ×10^{-7}	$^{20}Ne/^{22}Ne$	$^{22}Ne/^{21}Ne$	^{36}Ar ×10^{-7}	$^{36}Ar/^{38}Ar$	$^{40}Ar/^{36}Ar$	^{84}Kr ×10^{-9}	^{132}Xe ×10^{-9}
74002,175 (<0.1 cm)											
45-75 μm	7.12	23.7	60.7	58.4	12.59 ± .04	24.23 ± .41	71.0	5.128 ± .005	7.03 ± .10	5.69	10.7
<20 μm	7.25	125.	336.	347.	12.62 ± .04	30.73 ± .18	434.	5.238 ± .005	5.52 ± .02	25.7	39.2
74002,176 (0.5-1.0 cm)											
150-250 μm	13.26	26.2	64.5	70.7	12.59 ± .03	24.55 ± .32	122	5.147 ± .005	4.96 ± .03	8.32	13.6
<20 μm	10.81	155.	420.	412.	12.70 ± .03	31.27 ± .16	558	5.233 ± .005	4.53 ± .01	31.3	46.6
74002,177 (1.5-2.0 cm)											
150-250 μm	12.31	19.5	47.9	43.8	12.53 ± .14	23.04 ± .24	68.7	5.117 ± .005	6.45 ± .05	5.82	11.2
<20 μm	10.93	97.9	287.	284.	12.62 ± .03	30.79 ± .28	391.	5.250 ± .015	5.46 ± .02	21.2	32.5
74002,178 (3.0-3.5 cm)											
150-250 μm	13.53	4.08	7.42	5.72	11.88 ± .07	12.37 ± .36	13.2	4.965 ± .009	23.5 ± .4	2.85	8.74
<20 μm	11.47	45.7	124.	139.	12.55 ± .03	29.27 ± .34	176	5.317 ± .015	7.55 ± .05	9.43	15.0
74002,179 (5.0-5.5 cm)											
150-250 μm	14.20	1.89	1.85	1.71	9.28 ± .38	4.37 ± .46	2.12	3.907 ± .009	133. ± 8	0.86	2.71
<20 μm	11.42	20.4	56.1	81.4	12.39 ± .04	28.27 ± .75	97.2	5.286 ± .010	11.3 ± .2	5.35	10.7
20-45 μm											
Split B	2.41	3.32	4.87	7.30	11.36 ± .13	11.0 ± 1.0	8.8	4.65 ± .04	48.2 ± .7	5.91	15.2
Split D	5.54	5.89	12.4	13.4	11.57 ± .16	17.1 ± .4	12.5	4.99 ± .02	32.7 ± .3	1.60	2.57
74002,180 (12 cm)											
150-250 μm	9.70	1.72	1.43	1.30	7.76 ± .74	3.29 ± .65	1.65	3.62 ± .13	169. ± 16	1.13	3.79
<20 μm	13.78	13.8	36.7	60.5	12.31 ± .03	27.79 ± .45	70.6	5.17 ± .05	15.6 ± .2	6.02	15.1

Table 1. *(cont'd.)*

Sample	Wt.(mg)	^3He ×10^{-6}	^4He ×10^{-2}	^{22}Ne ×10^{-7}	$^{20}Ne/^{22}Ne$	$^{22}Ne/^{21}Ne$	^{36}Ar ×10^{-7}	$^{36}Ar/^{38}Ar$	$^{40}Ar/^{36}Ar$	^{84}Kr ×10^{-9}	^{132}Xe ×10^{-9}
74002,181 (18 cm)											
150-250 μm	9.32	1.56	1.26	0.94	6.41 ± 2.25	2.46 ± .64	0.99	3.06 ± .20	276 ± 22	1.13	4.17
<20 μm	12.18	8.06	19.4	39.6	12.25 ± .03	24.44 ± .10	49.5	5.146 ± .005	16.5 ± .1	2.75	5.66
74002,182 (26 cm)											
150-250 μm	10.15	1.51	1.10	0.65	3.16 ± 1.95	1.59 ± .56	0.63	2.33 ± .20	434 ± 50	0.48	1.50
<20 μm	11.63	4.44	9.52	17.6	12.02 ± .04	19.15 ± .18	27.3	5.292 ± .036	20.6 ± .2	1.75	3.77
74001,98 (32 cm)											
150-250 μm	13.12	2.15	2.06	1.17	7.95 ± .29	2.65 ± .26	1.61	3.35 ± .04	206 ± 5	5.49	1.89
<20 μm	10.68	21.9	52.7	47.1	12.71 ± .15	24.84 ± .42	99.3	5.185 ± .005	5.95 ± .07	12.0	2.88
74001,107 (37 cm)											
150-250 μm	12.95	1.91	1.79	1.17	7.73 ± .26	2.62 ± .19	2.00	3.60 ± .07	169 ± 7	6.00	2.16
<20 μm	10.74	4.08	7.87	11.1	11.90 ± .03	15.16 ± .26	22.9	5.14 ± .15	22.3 ± .5	3.91	1.21
74001,113 (44 cm)											
150-250 μm	10.25	1.19	0.98	0.65	6.31 ± 1.90	2.03 ± 2.5	0.62	3.57 ± .28	238 ± 46	1.88	0.63
90-150 μm	10.12	1.98	1.39	1.63	9.34 ± .24	3.56 ± .35	2.87	4.07 ± .41	95. ± 3	3.33	1.12
<20 μm	8.66	4.59	9.02	11.1	11.97 ± .07	13.46 ± .75	25.2	5.10 ± .03	21.3 ± .4	2.98	0.85
74001,119 (50 cm)											
150-250 μm	12.58	1.61	1.28	1.26	7.69 ± .30	2.66 ± .10	1.94	3.53 ± .06	183 ± 7	7.20	2.59
<20 μm	8.00	3.59	6.78	9.54	11.86 ± .18	14.24 ± .39	30.0	5.15 ± .03	21.6 ± .5	7.89	3.48
74001,125 (57 cm)											
150-250 μm	12.31	1.63	0.87	0.94	6.26 ± .67	1.99 ± .25	1.44	3.14 ± .09	175 ± 6	8.97	4.15
90-150 μm	10.83	2.60	0.88	0.84	1.68 ± 1.23	1.18 ± .18	0.65	1.59 ± .34	417 ± 43	2.06	1.02
20-45 μm	7.31	2.81	1.70	1.51	6.50 ± .65	2.05 ± .20	2.40	3.14 ± .06	131 ± 2	2.53	1.26
<20 μm	10.00	5.15	8.41	9.28	11.75 ± .03	9.83 ± .24	23.0	4.93 ± .03	18.6 ± .4	5.28	2.60
74001,2 (67 cm)											
150-250 μm	12.60	2.69	1.34	1.55	5.57 ± .51	1.84 ± .14	2.08	2.88 ± .06	132 ± 3	0.81	0.202
45-75 μm	12.50	13.2	2.14	1.81	6.94 ± .38	2.18 ± .18	2.47	3.14 ± .07	124 ± 3	1.51	0.42
<20 μm	9.74	4.15	5.95	6.88	11.24 ± .06	7.48 ± .23	14.8	4.77 ± .02	25.8 ± .3	2.32	0.57

Table 1. From Bogard and Hirsch (1978).